Biomed Microdevices (2014) 16:567–573
DOI 10.1007/s10544-014-9859-z

Controlled ultrasonic micro-dissection of thin tissue sections

Changhai Ru · Jun Liu · Ming Pang · Yu Sun

Published online: 10 April 2014

Abstract In order to obtain sufficient quantities of pure populations of cells or a single cell from surrounding tissue for analytical investigation, we have developed an ultrasonic microdissection system. The system utilizes a vision-based method for detecting the contact between the microdissection needle tip and a target surface. A multilayer stack piezoelectric actuator is employed to generate ultrasonic vibrations for histological isolation. Automated micro-dissection is also realized using visual feedback and vision-based control. Experimental results on tumor tissue sections show that the system has a high dissection accuracy and efficiency and is able to realize dissecting arbitrary shapes in specified locations on a tissue sample. Furthermore, effects in variations of vibration amplitude and frequency of ultrasonic micro-dissection as well as needle insertion depths on micro-dissection accuracy and speed were evaluated.

Keywords Piezoelectric actuator · Ultrasonic vibration · Depth control · Tissue microdissection · Parameter selection

C. Ru (✉) · M. Pang · Y. Sun (✉)
College of Automation, Harbin Engineering University, Harbin 150001, China
e-mail: rchhai@gmail.com
e-mail: sun@mie.utoronto.ca

C. Ru · Y. Sun
Jiangsu Provincial Key Laboratory of Advanced Robotics & Collaborative Innovation Center of Suzhou Nano Science and Technology, Soochow University, Suzhou, China 215000

J. Liu · Y. Sun
Department of Mechanical and Industrial Engineering, University of Toronto, Toronto, ON M5S 3G8, Canada

1 Introduction

In modern pathology, the extraction of cells from a tissue sample is a necessary step for molecular analysis of small cell clusters (Ichikawa et al. 2011; Deeken et al. 2008). Because cells in a complex tissue biochemically and biophysically interact with surrounding cells, accurate analysis of gene expression patterns in disease progression demand the procuring of sufficient quantities of pure populations of target cells from a tissue sample (Deeken et al. 2008; Harsch et al. 2001). Micro-dissection involves cutting through a thin tissue section, which is a few micrometers thick, separating the target group of cells from the tissue, and collecting the dissected cells for subsequent pathological analysis.

A number of micro-dissection methods have been developed, including manual cutting, mechanical auxiliary micro-dissection, laser capture, and piezo-power micro-dissection (PPMD) (Ishii et al. 2005; Chen et al. 2010; Terpitz and Zimmermann 2010; Harsch et al. 2001; Brandt et al. 2003). Manual cutting is time consuming and has low accuracy and poor repeatability. It is based on trial and error and is only applicable to large-area dissection. Mechanical auxiliary is assisted by a micromanipulator that guides a needle to scrape off an area of interest from a thin tissue section. While positioning accuracy is improved, it is still highly operator skill dependent. More importantly, without laser power or mechanical vibration, the efficiency of cleanly separating a cell or a small group of cells from the tissue sample is low.

Laser catapulting is a powerful technique for isolating and capturing cells from microscopic regions of tissue, cells or organisms. However, the laser system needs a high cost of equipment, requires special membranes to view intact cell and induces a potential destruction of cells during procurement. In comparison, PPMD uses an ultrasonic oscillating cutting tool to induce low-amplitude, high-frequency vibration to a fine metal tip to excise selected cell areas from tissue sections

(Harsch et al. 2001). After cutting, the isolated sample is collected using a standard aspiration pipette. The efficiency of PPMD in generating pure samples for differential gene expression has been demonstrated. In addition, it has been shown to be comparable to laser micro-dissection in terms of tissue preparation time, speed and precision of micro-dissection. Without laser heat and infra-red radiation, the technique is also free of inducing cell and tissue sample damage (McLachlan et al. 2003).

However, parameter selections of PPMD operation, such as vibration amplitude and frequency, are presently based on trial and error. These parameters are critical for effectively isolate target cell areas from a tissue section. Furthermore, insertion depth into a tissue section, which significantly determines the accuracy of tissue dissection and the cleanliness of cutting features within the tissue section, is empirically conducted. Micro-dissection needle tip is also often broken due to poor penetration depth control.

This work, for the first time, investigates the selection of amplitude and frequency of ultrasonic micro-dissection. The effects of cutting speed and needle insertion depth on micro-dissection accuracy are also studied. Experiments on tumor tissue sections were conducted to obtain parameter selection guidelines.

2 System setup

As shown in Fig. 1, the system consists of (1) a host computer, (2) inverted microscope (Ti-E, Nikon), (3) motorized micro-manipulators (MP285, Sutter), (4) pipette holder, (5) piezo-electric actuator, (6) tissue section, (7) a CMOS camera (A601f, Basler), (8) a motorized *X-Y* translational stage (ProScan II, Prior), (9) syringe pump (PHD ULTRA™), (10) lead screw, (11) a 25-microliter glass syringe (Hamilton), (12) mounting rack, (13) micromanipulator controller, (14) signal generator and a custom developed piezoelectric actuator power supply based on PA92 (Apex Microtechnology), (15) controller for translational stage, and (16) vibration isolation table. The microdissection needle is made of tungsten with high hardness and low coefficient of friction. Sharpness and hardness make the needles effective for cell dissection. Standard tissue dissection needles made of Tungsten are used, with a tip diameter of 5 um. A high dynamic stack piezoelectric actuator (PSt VS9, Piezomechanik) is used, whose maximum stroke length is 7 μm, stiffness is 25 N/μm, and resonant frequency is 40 kHz in Fig. 1b.

3 Ultrasonic micro-dissection

Figure 2 illustrates the dissection model. With a sinusoidal driving signal, the dissection needle is vibrated, generating

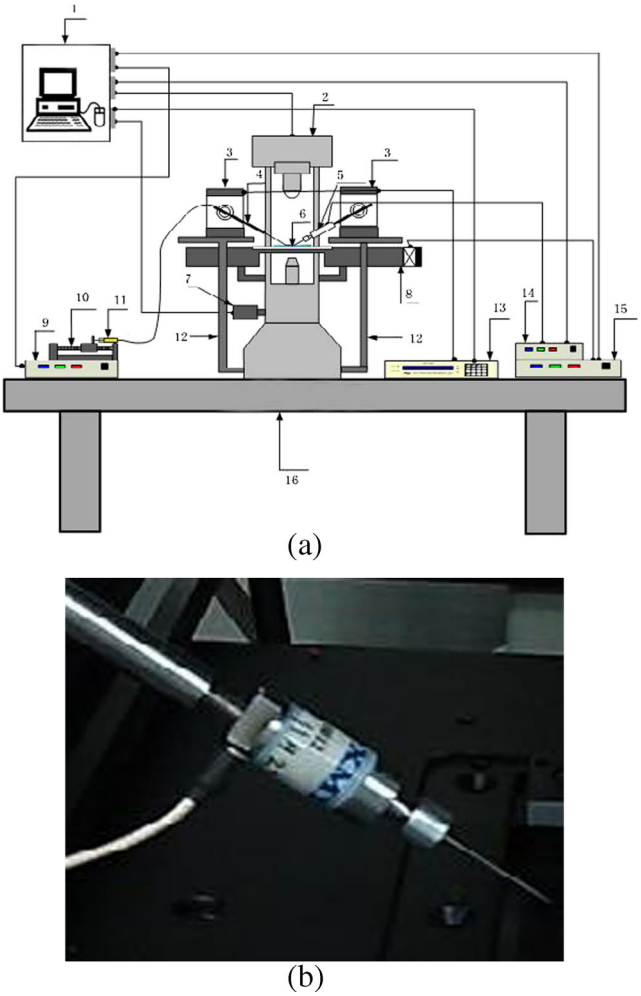

Fig. 1 **a** System setup for micro-dissection of thin tissue sections **b** Stack piezoelectric actuator

two components along the X and Z axes

$$x(t) = A\sin(\omega t) * \cos(\theta) \tag{1}$$

$$z(t) = A\sin(\omega t) * \sin(\theta) \tag{2}$$

with a vibration velocity

$$v(t) = A\omega * \cos(\omega t) \tag{3}$$

The relative speed, v(r) between the dissection needle and tissue section is the movement speed of the micromanipulator, v(m) combined with the vibration speed, v(t), as illustrated in Fig. 3,

$$v(r) = v(m) + v(t) = v(m) + A\omega * \cos(\omega t) \tag{4}$$

where ω is the vibration frequency (ω=2πf), and A is the maximal amplitude. In Fig. 2, H is the tissue section thickness; h_2 is the insertion depth of the dissection needle, θ is the

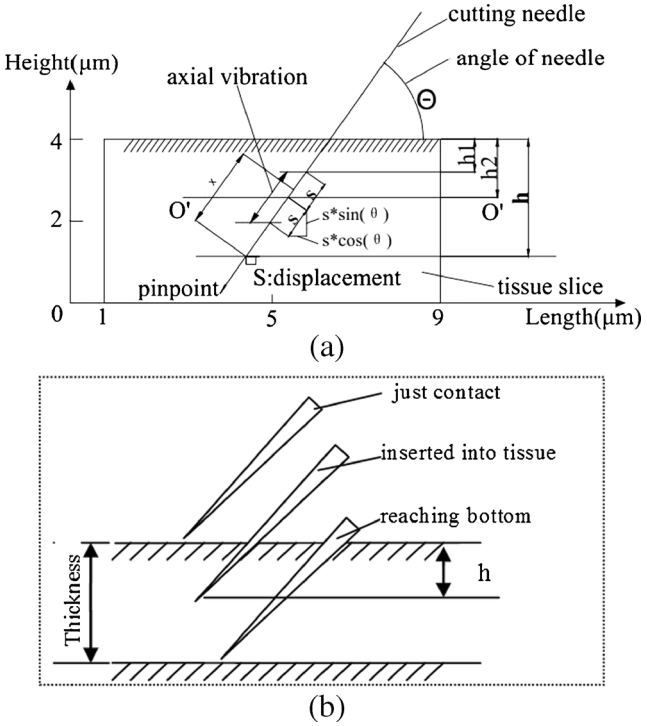

Fig. 2 **a** Micro-dissection model **b** Needle tip at different height into the tissue section

entering angle of the needle, and S is the needle tip's displacement.

As show in Fig. 2b, when the needle tip just contacts the tissue section, vibration energy cannot spread effectively to isolate the tissue. Inserting the needle tip relatively shallow into the tissue section can also produce ineffective dissection results because the vibration energy cannot be transmitted all the way to the bottom of the tissue section, resulting in incomplete dissection. Inserting the needle to a proper depth enables the vibration energy to be delivered throughout the tissue section for effective dissection. Penetration depth must be well controlled; otherwise, the fragile needle tip can be damaged when it vibrates on the sample substrate. Therefore, depth control in ultrasonic micro-dissection is crucial.

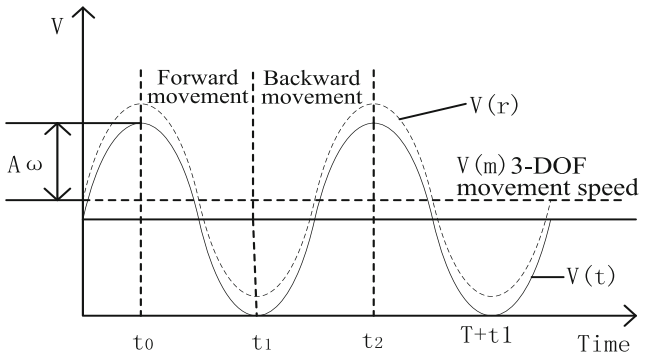

Fig. 3 Relative speed between micro-dissection needle and tissue section

4 Depth detection

Accurately controlling the needle tip position along the Z-axis is important in micro and nano manipulation (Shamoto and Moriwaki 1994; Fukuda et al. 2003; Aoki et al. 2003; Eichhorn et al. 2008). In order to attain position information of the needle tip in the Z direction, touch/force sensors have been developed and used for detecting the contact between the needle tip and the substrate or object (Haitjema et al. 2001; Trummer et al. 2004; Chawda and O'Malley 2011; Sitti and Hashimoto 2000). In this work, a computer vision-based contact detection approach (Wang et al. 2007) is used for determining the relative vertical positions between the needle tip and tissue. Using microscopy visual feedback, the micro-dissection needle tip is visually tracked in real time. When the needle is lowered and contacts substrate surface, further motion of the needle in the *Z* direction causes the needle to slide on the target surface, a phenomenon detectable from image processing. Prompt detection of the slight horizontal sliding motion enables the system to detect contact effectively and lift the microdissection needle upwards above the sample, thus avoiding sample damage.

4.1 Visual tracking of micro-dissection needle tip

To obtain accurate positions of the micro-dissection needle tip, it needs to be identified and tracked. An ROI (region of interest) containing the needle tip is obtained via operator's mouse clicking near the needle tip. The micro-dissection probe is a tungsten probe (5 μm) mounted onto the piezoelectric actuator. After Gaussian filtering, adaptive thresholding, and morphological operations, the contour of the needle tip is obtained. The needle is then controlled to move downwards along the Z direction to establish contact with the substrate surface.

4.2 Contact detection

Figure 4 shows an image plane, objective lens, the dissection needle, and the sample surface. when the needle is driven by the micromanipulator to move downwards at a constant step displacement (0.5 μm/step), the initial position of needle tip, the position before contact, exact contact position, and position after contact are denoted, respectively as position 1, 2, 3, and 4 in the world frame and 1′, 2′, 3′, and 4′ in the image plane. The distance between the tip at initial position 1 and the target surface is denoted by *h*; the distance between the tip of the needle at position 1 and the objective lens is *u*; and the distance between the image plane and the objective lens is *v*. The horizontal distance between the tip and the optical coordinate, before contact is denoted by X_0, and denoted by X after contact.

Before contact is established, similarity of triangles gives

$$\frac{x}{X_0} = \frac{v}{u-Z} \tag{5}$$

Differentiating both sides yields

$$dx = \frac{v \cdot X_0}{u^2} dZ \tag{6}$$

Before the needle tip and the target surface make contact, the x coordinate values of the tip decreases in proportion to downward displacements along the Z direction in the world frame. Similarly, after contact is formed according to Fig. 4b, c

$$\frac{x}{X_0 + tg\frac{\theta}{2}(Z-h)} = \frac{v}{h} \tag{7}$$

Differentiating both sides yields

$$dx = -\frac{v \cdot tg\left(\theta/2\right)}{h} dZ \tag{8}$$

It implies that after contact, the x coordinate values of the tip increases in proportion to downward displacements along the Z direction in the world frame.

In summary, the x-coordinate values of the needle tip in the image plane decreases before contact and then increases after contact. When the needle tip reaches the minimal x-coordinate value in the image plane, initial contact occurs between the needle tip and the target surface. Thus, the relative vertical position between the needle tip and target surface is determined by monitoring the pattern change in the x-coordinate values of the needle tip.

In the contact detection process, when the micro-dissection needle descends towards the tissue substrate, the rightmost position of the needle tip is tracked in real time (Fig. 4d). During the downward motion 1′-2′-3′, the needle approaches the substrate surface at a speed of 0.5 μm/step without contact. The needle tip slides on the substrate surface (during the process 3′-4′) during further downward motion, when contact is detected. The needle tip then stops moving downwards and begins to retract (process 4′-3″-5′) until a specified height above the substrate.

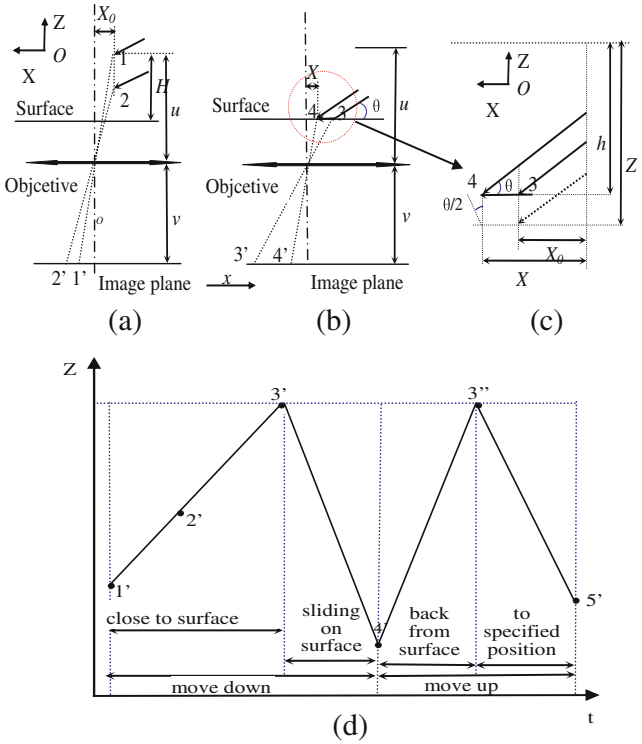

Fig. 4 Contact detection based on computer vision

5 Experimental results and discussion

In our experiments, rectal tumor tissue sections (5 μm thick) were used. The system conducted contact detection first. It then inserted the dissection needle at different depths into the tissue sections and applied different dissection parameters.

The first experiment involved direct dissection without using ultrasonic vibration. Although the micromanipulator accurately positioned the dissection needle (tip diameter: 5 μm), connections of the target area were difficult to cleanly separately from the rest of the tissue section, hence, resulting in irregular and wide lines (see Fig. 5). In comparison, ultrasonic vibration without parameter optimization produced much more accurate and regular dissection results.

We then experimented with different parameters and quantified tissue dissection results. Critical parameters determining dissection performance include driving voltage amplitude, driving frequency, depth of dissection, and cutting speed. Regularity of dissected lines is measured by quantifying the sum of squared errors (SSE) of the distance between each point on the line edge to the center line, as shown in Fig. 6. The SSE to the center line, as shown in Fig. 6, was defined as a quality measure. A thin and regular dissected line results in a low SSE value, and a high SSE value indicates poorer dissection quality. SSE equaling zero means perfect regularity of dissected lines.

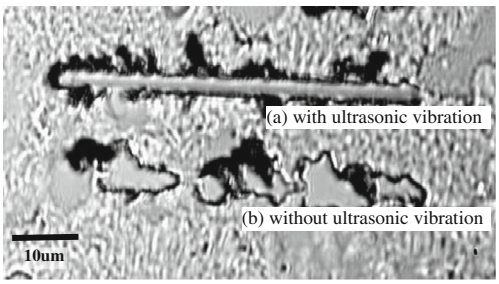

Fig. 5 Tissue micro-dissection with and without ultrasonic vibration

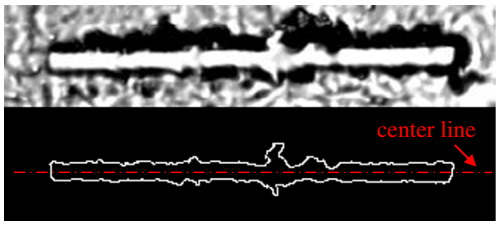

Fig. 6 Sum of squared errors (SSE) to the center line is defined to measure dissection quality/regularity

The experimental results show that, with higher driving voltage amplitudes (e.g., 15 V vs. 30 V as shown in Fig. 7a), high energy was transferred from the dissection needle tip though the entire tissue section, resulting in a clean cutting line (i.e., low SSE value). However, too high a driving voltage produced too large vibration amplitudes, increasing the risk of needle tip damage when touching the substrate and hence, requiring more accurate Z positioning control. At an amplitude of 15 V, the vibration amplitude of the dissection needle tip was measured via laser interferometer to be 0.58 μm.

When driving frequency was increased, dissection quality was improved. Since ultrasonic energy is proportional to the driving frequency, a higher driving frequency produces higher energy, which facilitates tissue dissection. Data shown in Fig. 7b were collected with a fixed driving voltage amplitude of 20 V.

The cutting speed and insert depth were also proven crucial for ultrasonic dissection. At higher cutting speed (i.e., micromanipulator speed), the time for energy from the dissection needle tip to transmit to the tissue section becomes shorter. As shown in Fig. 7c, when the cutting speed was higher than >100 μm/s, cutting lines became irregular and SSE value increased significantly. At a cutting speed higher than 100 μm/s, dissection failures occurred because the target area was not separated from the rest of the tissue section.

As introduced in Section IV, our system detects the contact between the dissection needle and substrate using a computer vision approach. The visual contact detection approach together with the sub-micrometer resolution of the motorized micromanipulator enabled the system to control needle insertion depth with the accuracy better than 1 μm. Figure 7d shows the dissection quality at a needle insertion depth of 0 μm, 1 μm, and 2 μm into the tissue section.

The insertion depth of 0 μm refers to the situation where the needle tip just contacted the surface of the tissue section. The extremely small insertion depth and the unevenness of the sample caused intermittent interactions between the needle tip and the sample, which only produced a shallow line on the surface of tissue section in Fig. 8a. When the needle was inserted into the tissue section by 1 μm, the 5 μm thick tissue section was not completed separately along the cutting line because vibration energy cannot be transmitted throughout the tissue section. At an insertion depth of 2 μm, clean and regular dissection was achieved consistently. Complete isolation was realized by using a micropipette to remove a dissected area (see Fig. 8c, e).

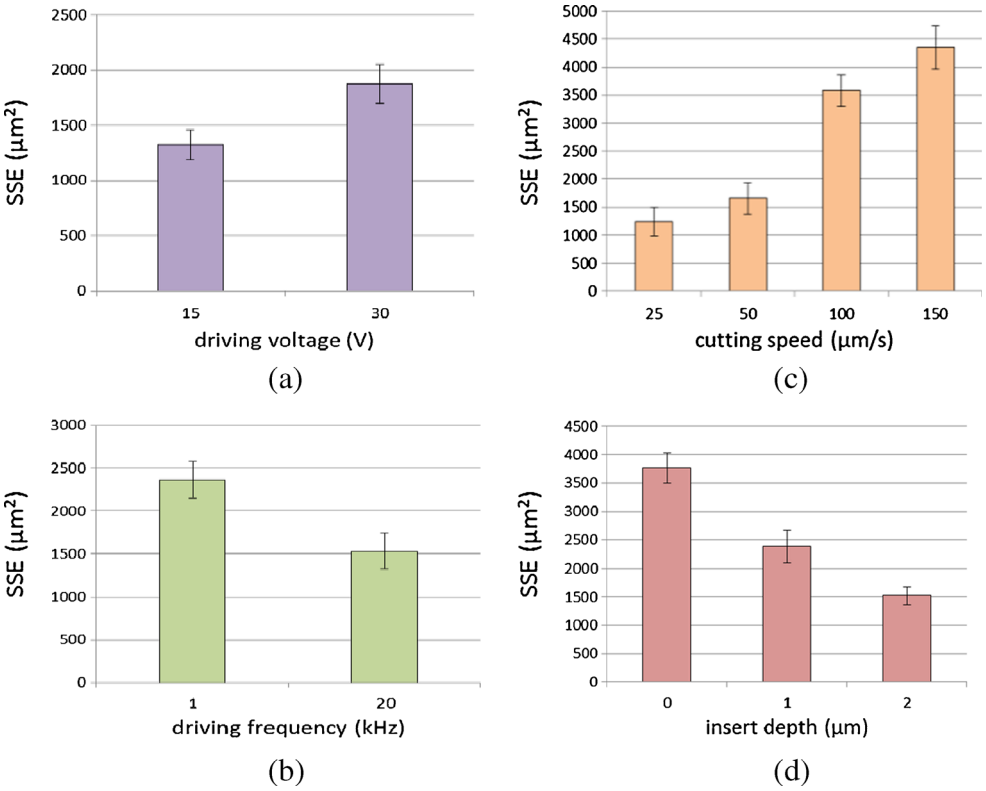

Fig. 7 Effect of different parameters on tissue dissection (n=5, five trials for each parameter). **a** voltage amplitude, **b** voltage frequency, **c** cutting speed, and **d** needle insertion depth

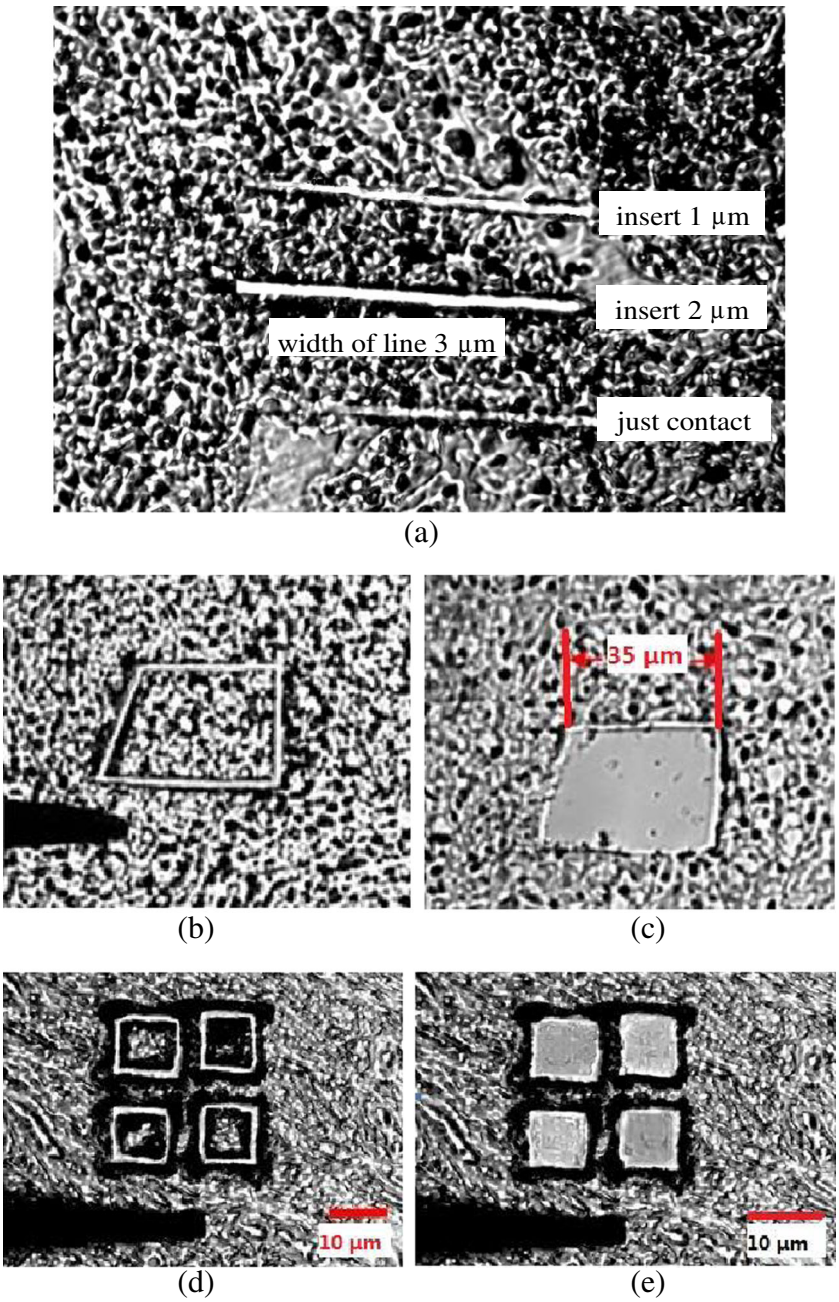

Fig. 8 **a** Dissection results vary with different needle insertoion depth into the tissue section. **b** Dissect a quadrangled area. **c** Remove the quadrangled area. **d** Dissect an array of squares. **e** Remove the array

Based on these experimental results, dissection parameters set in our system were 20 V in driving voltage amplitude, 20 kHz in driving frequency, cutting speed of 50 µm/s, and needle insertion depth of approximately half way into the tissue section (e.g., 2–3 µm into tissue sections that are 5 µm thick). The system enables micro-dissection using computer mouse clicking. An operator draws lines to indicate target areas for dissection. The system positions the dissection tip using visual servo control in the XY plane and controls insertion depth into the tissue based on contact detection results. Figure 8c and e shows examples of dissection and removal of target areas.

6 Conclusion

This paper presented controlled ultrasonic micro-dissection of thin tissue sections. The system is capable of controlling a number of parameters, such as insertion depth of the needle tip into the tissue section and vibration amplitude and frequency. Through parameter evaluation, the effect of these parameters on microdissection results was evaluated. Automated micro-dissection was realized via visual feedback and vision-based control. Experimental results on tumor tissue sections show that the system has a high dissection accuracy and efficiency and is able to realize dissecting arbitrary shapes in specified locations on a tissue sample.

Acknowledgments This work was financially supported by National Natural Science of China (Grant No. 61233010), Instrument Development Major Program of National Natural Science of China (Grant No. 61327811), Jiangsu Natural Science Founds for Distinguished Young Scholar (Grant No. BK2012005), and Qing Lan Project of Jiangsu Province.

References

K. Aoki, H.T. Miyazaki, H. Hirayama, K. Inoshita, T. Baba, K. Sakoda, N. Shinya, Y. Aoyagi, Microassembly of semiconductor threedimensional photonic crystals. Nat. Mater. **2**(2), 117–121 (2003)

S. Brandt, C. Walz, M. Schad, N. Pavlovic, J. Kehr, A simple, chisel-assisted mechanical microdissection system for harvesting homogeneous plant tissue suitable for the analysis of nucleic acids and proteins. Plant Mol. Biol. Report. **21**, 417–427 (2003)

V. Chawda, M.K. O'Malley, Vision-based force sensing for nanomanipulation. IEEE/ASME Trans. Mechatron. **16**, 1171–1183 (2011)

L. Chen, C. Ru, W. Rong, Y. Liu, L. Sun, Design, modeling and control of a piezoelectric ultrasonic microdissection technique for the molecular analysis of tissue. Smart Mater. Struct. **19**, 025003 (2010)

R. Deeken, P. Ache, I. Kajahn, J. Klinkenberg, G. Bringmann, R. Hedrich, Identification of Arabidopsis thaliana phloem RNAs provides a search criterion for phloem-based transcripts hidden in complex datasets of microarray experiments. Plant J. **55**, 746–759 (2008)

V. Eichhorn, S. Fatikow, T. Wich, C. Dahmen, T. Sievers, K. Andersen, K. Carlson, P. Bggild, Depth-detection methods for microgripper based cnt manipulation in a scanning electron microscope. J. Micro-Nano Mechatron. **4**(1), 27–36 (2008)

T. Fukuda, F. Arai, L. Dong, Assembly of nanodevices with carbon nanotubes through nanorobotic manipulations. Proc. IEEE **91**(11), 1803–1818 (2003)

H. Haitjema, W. Pril, P.H.J. Schellekens, A silicon-etched needle for 3-D coordinate measurements with an uncertainty below 0.1 um. IEEE Trans. Instrum. Meas. **50**(6), 1519–1523 (2001)

M. Harsch, K. Bendrat, G. Hofmeier, D. Branscheid, A. Niendorf, A new method for histological microdissection utilizing an ultrasonically oscillating needle: demonstrated by differential mRNA expression in human lung carcinoma tissue. Am. J. Pathol. **158**, 1985–1990 (2001)

A. Ichikawa, T. Tanikawa, S. Akagi, K. Ohba, Automatic cell cutting by high-precision microfluidic control. J. Robot. Mechatron. **23**(1), (2011)

H.A. Ishii, G.A. Graham, A.T. Kearsley, P.G. Grant, C.J. Snead, J.P. Bradley, Rapid extraction of dust impact tracks from silica aerogel by ultrasonic microblades. Meteorit. Planet. Sci. **40**, 1741–1747 (2005)

J.L. McLachlan, A.J. Smith, P.R. Cooper, Piezo-power microdissection of mature human dental tissue. Arch. Oral Biol. **48**, 731–736 (2003)

E. Shamoto, T. Moriwaki, Study on elliptical vibration cutting. Ann. CIRP **43/1**, 35–38 (1994)

M. Sitti, H. Hashimoto, Two-dimensional fine particle positioning under optical microscope using a piezoresistive cantilever as a manipulator. J. Micromechatronics **1**(1), 25–48 (2000)

U. Terpitz, D. Zimmermann, Isolation of guard cells from fresh epidermis using a piezo-power microdissection system with vibration attenuated needles. BioTechniques **48**(1), 68–70 (2010)

G. Trummer, C. Kurzals, R. Gehring, D. Leistner, Next-generation proximity and position sensors. Sensors **21**(3), 14–21 (2004)

W.H. Wang, X.Y. Liu, Y. Sun, Contact detection in microrobotic manipulation. Int. J. Robot. Res. **26**(8), 821–828 (2007)